# Electronic, Infrared, and Resonance-Raman Spectroscopic Studies of the Linear-chain, Halogen-bridged, Mixed-valence Complexes $[Pt(NH_3)_4][Pt(NH_3)_4X_2]Y_4$ (X = Br or I, Y = $HSO_4$, $ClO_4$, or $BF_4$). The *X*-Ray Crystal Structures of $[Pt(NH_3)_4][Pt(NH_3)_4Br_2][HSO_4]_4$ and $[Pt(NH_3)_4][Pt(NH_3)_4I_2][HSO_4]_3[OH]\cdot H_2O$ †

**Robin J. H. Clark * and Mohamedally Kurmoo**
*Christopher Ingold Laboratories, University College London, 20 Gordon Street, London WC1H 0AJ*
**Anita M. R. Galas and Michael B. Hursthouse**
*Department of Chemistry, Queen Mary College, Mile End Road, London E1 4NS*

The complexes $[Pt(NH_3)_4][Pt(NH_3)_4Br_2]Y_4$, Y = $HSO_4$, $ClO_4$, or $BF_4$, and $[Pt(NH_3)_4][Pt(NH_3)_4I_2]$-$[HSO_4]_3[OH]\cdot H_2O$ have been prepared by partial aerial oxidation of Magnus green in 50% $H_2SO_4$ in the presence of KBr or KI as appropriate. The complexes are deeply coloured and highly dichroic, as is typical of linear-chain, halogen-bridged species. The crystal structures of the two $[HSO_4]^-$ salts have been refined within the space groups $P2_1/c$ ($Z$ = 1) for the bromide and *Pmcn* ($Z$ = 4) for the iodide to final $R$ factors of 0.0373 and 0.0484, respectively. In the case of the bromide, the $[Pt^{II}(NH_3)_4][Pt^{IV}(NH_3)_4Br_2]$ chains are longitudinally disordered so that all the Pt atom sites comprise $\frac{1}{2}Pt^{II} + \frac{1}{2}Pt^{IV}$ and the axial bromine atoms half-occupy two positions 0.559 Å apart; the key bond lengths are $Pt^{IV}$–Br 2.467 Å and $Pt^{II}$–Br 3.022 Å. The $Pt^{II}N_4$ and $Pt^{IV}N_4$ square planes are eclipsed when viewed down the chain axis. In the case of the iodide, the $[Pt^{II}(NH_3)_4][Pt^{IV}(NH_3)_4I_2]$ chains are completely ordered, with the bridging iodine atoms occupying only one site; the $Pt^{IV}$–I and $Pt^{II}$–I distances are 2.686 and 3.148 Å, respectively. The $Pt^{II}N_4$ and $Pt^{IV}N_4$ square planes are, in this case, staggered by 46° when viewed down the chain axis. The intense resonance-Raman spectra of the complexes, obtained by irradiating within the contours of their $Pt^{IV} \leftarrow Pt^{II}$ intervalence bands, are dominated by progressions (at most to 14 members) in the axial, totally symmetric, chain-stretching mode, $\nu_1$, $\nu_{sym}(X-Pt^{IV}-X)$, as shown by polarisation and intensity studies. The results are discussed with respect to related ones for other localised mixed-valence complexes.

Considerable work has been devoted recently to the syntheses [1-5] and characterisation of semi-conducting and highly conducting one-dimensional materials. Much of this work has been focused on complexes of platinum and palladium owing to the ability of these elements to form long-chain polymers made up of stacks of metal atoms in square-planar co-ordination. In general, two kinds of chain structures are observed, namely those containing direct metal–metal interaction and those containing metal atoms bridged by halogen atoms.

The formulations and structures of the complexes formed by partial aerial oxidation of Magnus green, $[Pt(NH_3)_4]$-$[PtCl_4]$, in 50% sulphuric acid are controversial, as outlined at a recent NATO conference.[6] We have now succeeded in isolating from these mixtures, in the presence of KBr, the Reihlen's-green-type analogues $[Pt^{II}(NH_3)_4][Pt^{IV}(NH_3)_4Br_2]$-$[HSO_4]_4$ (see also ref. 7), and the analogous perchlorate and tetrafluoroborate salts. We have also isolated and characterised the complex $[Pt^{II}(NH_3)_4][Pt^{IV}(NH_3)_4I_2][HSO_4]_3[OH]\cdot H_2O$. The spectroscopic results on the complexes, which imply that they are halogen-bridged mixed-valence complexes of platinum, have been confirmed by single-crystal *X*-ray diffraction studies on the two bisulphate salts, thus for the first time placing the structures of two key complexes from this system onto a firm basis.

† *catena*-Tetra-ammine-μ-bromo-platinum(II,IV) tetrakis(hydrogensulphate) and *catena*-tetra-ammine-μ-iodo-platinum(II,IV) tris-(hydrogensulphate) hydroxide monohydrate.

*Supplementary data available* (No. SUP 23416, 23 pp.): thermal parameters, structure factors. See Notices to Authors No. 7, *J. Chem. Soc., Dalton Trans.*, 1981, Index issue.

## Experimental

*Preparation of Complexes.*—The salt $[Pt(NH_3)_4][Pt(NH_3)_4$-$Br_2][HSO_4]_4$ was isolated as gold-green needles by allowing a hot solution of Magnus green dissolved in 50% sulphuric acid to cool, in the presence of an excess of KBr, slowly to room temperature. It can also be obtained by adding sulphuric acid slowly to a suspension of equimolar quantities of $[Pt(NH_3)_4]Br_2$ and $[Pt(NH_3)_4Br_2]Br_2$ (Found: H, 2.60; Br, 15.1; N, 10.4; S, 11.5. $H_{28}Br_2N_8O_{16}Pt_2S_4$ requires H, 2.65; Br, 14.85; N, 10.4; S, 11.95%).

Reaction of $[Pt(NH_3)_4]Cl_2$ and $[Pt(NH_3)_4Br_2]Br_2$ in equimolar amounts in 50% $HClO_4$ or 42% $HBF_4$ at 60 °C yields the complexes $[Pt(NH_3)_4][Pt(NH_3)_4Br_2]Y_4$, Y = $ClO_4$ or $BF_4$, respectively. In both cases, the crystals are green-gold.

Some difficulty was experienced in the synthesis of the analogous iodo-complex, since several of the obvious routes apparently led to the formation of impure products. The most satisfactory route was as follows. Magnus green was dissolved in a hot solution of 50% sulphuric acid; on cooling, orange-red crystals of the chloro-complex $[Pt(NH_3)_4][Pt(NH_3)_4Cl_2]$-$[HSO_4]_4$ separated out. These were then dissolved in water, KI added, followed by concentrated $H_2SO_4$ until the $H_2O$ : $H_2SO_4$ ratio was 1 : 1. The solution was then allowed to cool overnight, whereupon green-brown crystals of the corresponding iodo-complex separated out. The yield was very low, and insufficient complex was obtained to establish analytically the precise composition of the anion, *cf.* later comments of a crystallographic nature.

*Spectroscopic Details.*—Electronic spectra of the complexes were recorded by transmission through Nujol mulls or pressed discs using a Cary 14 spectrometer, or by diffuse

reflectance using a Cary 14 or a Unicam 800 spectrometer.

Infrared spectra were recorded as Nujol mulls using a Perkin-Elmer 225 spectrometer (4 000—200 $cm^{-1}$) and a Nicolet 7199 interferometer (400—50 $cm^{-1}$) (courtesy of Dr. P. Goggin, Bristol).

Raman spectra were recorded using Spex 1401 or 14018 (R6) double monochromators equipped with Bausch and Lomb gratings (1 200 line $mm^{-1}$) and Jobin–Yvon holographic gratings (1 800 line $mm^{-1}$), respectively. Coherent Radiation model CR3 $Ar^+$ and $Kr^+$ lasers provided the appropriate exciting lines. Photon-counting techniques were employed for detection, using cooled RCA C31034 photomultipliers. Spectra at room temperature were recorded using the rotating-sample technique [8,9] and at liquid-nitrogen temperature using an appropriate Dewar assembly. A cylindrical lens was used to line-focus the laser beam and thus prevent local heating and decomposition of the samples.

Excitation profiles and intensities were measured relative to that of the $a_1$ band of sulphate and corrected for the response of the instrument. Wavenumbers of bands were calibrated with respect to the emission lines of neon.

*Crystallographic Details.*—Crystals of the $[HSO_4]^-$ salts of both the bromide and iodide were examined in detail by single-crystal *X*-ray photography in order to establish the correct unit cell. In neither case was any diffuse reflection detected, although for the iodide we noted that the $h = 2n + 1$ layers were very weak and showed some streaking, and that the $h = 4n$ layers were much stronger than the other even layers.

Crystal mounting, cell determination and refinement, and data collection followed normal procedures.[10] It is interesting to note that the automatic search routine in the Nonius CAD 4 software found the correct cell for the iodide, in spite of the uneven intensity distribution.

*Crystal data.* $[Pt(NH_3)_4][Pt(NH_3)_4Br_2][HSO_4]_4$: $M = 1\,074.51$, Monoclinic, $a = 5.489(1)$, $b = 10.339(1)$, $c = 10.648(1)$ Å, $\beta = 92.57(1)°$, $U = 603.7$ Å$^3$, space group $P2_1/c$, $Z = 1$, $D_c = 2.95$ g $cm^{-3}$, $\mu$(Mo-$K_\alpha$) = 147.7 $cm^{-1}$, $F(000) = 1\,004$.

$[Pt(NH_3)_4][Pt(NH_3)_4I_2][HSO_4]_3[OH]\cdot H_2O$: $M = 1\,106.44$, Orthorhombic, $a = 11.667(3)$, $b = 14.319(2)$, $c = 15.374(1)$ Å, $U = 2\,568.3$ Å$^3$, space group $Pmcn$, $Z = 4$, $D_c = 2.86$ g $cm^{-3}$, $\mu$(Mo-$K_\alpha$) = 130.0 $cm^{-1}$, $F(000) = 1\,016$.

*Data collection.* A Nonius CAD 4 diffractometer and graphite-monochromated Mo-$K_\alpha$ radiation ($\lambda = 0.710\,69$ Å) were employed in the $\omega$—$2\theta$ scan mode.[10]

$[Pt(NH_3)_4][Pt(NH_3)_4Br_2][HSO_4]_4$: crystal size $0.06 \times 0.06 \times 0.265$ mm, faces $\{01\bar{1}\}$, $\{011\}$, and $\{100\}$; 2 053 data measured, giving 1 749 unique of which 1 288 were observed [$I > 1.5\,\sigma(I)$].

$[Pt(NH_3)_4][Pt(NH_3)_4I_2][HSO_4]_3[OH]\cdot H_2O$: crystal size $0.206 \times 0.113 \times 0.088$ mm, faces $\{100\}$, $\{0\bar{1}1\}$, and $\{011\}$; 2 642 data measured, 2 327 unique, and 1 652 observed [$I > 1.5\,\sigma(I)$]. Both sets of data were corrected for absorption.

*Structure determination and refinement.* The structure of the bromide was solved and refined without problems by standard methods. The iodide structure analysis was quite problematic. In the final structure, in *Pmcn*, with the platinum and iodine atoms sited on mirror planes, the asymmetric unit contains one well ordered and refined $[HSO_4]^-$ group [involving atom S(1)] and one group involving S(2) which appears to be disordered, with reduced average occupancy, and which also seems to be associated with two additional single atoms, possibly an oxygen atom of an $[OH]^-$ group and a water molecule. Occupancy of $\frac{1}{2}([HSO_4]^- + [OH]^-)$ at each equivalent position gives the required charge balancing.

We attempted to remove the disorder by refining the structure in the non-centrosymmetric space group $P2_1cn$, but no stable, refinable model could be found. Accordingly we have settled on the model presented, and feel that the low *R* value (see below), reasonable anisotropic thermal parameters for all atoms except the disordered ' $SO_4H\cdot OH$ ' unit, and the bond lengths and angles found indicate the model to be reliable.

The final *R* and *R'* values are 0.0373, 0.0358 for the bromide and 0.0484, 0.0513 for the iodide. Final atomic fractional co-ordinates are given in Table 1. Computers, programs, and sources of scattering factor data are as given in ref. 10.

**Table 1.** Atom co-ordinates ($\times 10^4$)

| Atom | *x* | *y* | *z* |
|---|---|---|---|
| (*a*) The bromide | | | |
| Pt | 0 | 0 | 0 |
| Br | 4 494(3) | −29(3) | 4(2) |
| N(1) | 322(12) | 1 899(6) | 526(7) |
| N(2) | −131(13) | 546(7) | −1 854(5) |
| S | 5 298(3) | 1 393(2) | 3 561(2) |
| O(1) | 5 541(21) | −86(5) | 3 297(8) |
| O(2) | 7 172(10) | 2 000(6) | 2 876(5) |
| O(3) | 5 810(15) | 1 583(7) | 4 939(5) |
| O(4) | 2 855(10) | 1 780(6) | 3 187(6) |
| (*b*) The iodide | | | |
| Pt(1) | 2 500 | 2 043(1) | 1 642(1) |
| Pt(2) | 7 500 | 2 029(1) | 1 674(1) |
| I(1) | 9 802(1) | 2 046(1) | 1 655(1) |
| S(1) | 9 608(4) | 1 036(4) | −1 109(3) |
| S(2) | 4 587(16) | 847(17) | 4 406(12) |
| N(11) | 2 500 | 3 243(19) | 965(19) |
| N(12) | 2 500 | 876(22) | 2 376(19) |
| N(13) | 2 500 | 2 819(18) | 2 787(17) |
| N(14) | 2 500 | 1 304(19) | 467(17) |
| N(21) | 7 500 | 596(17) | 1 334(19) |
| N(22) | 7 500 | 3 431(17) | 1 986(15) |
| N(23) | 7 500 | 1 760(21) | 2 985(15) |
| N(24) | 7 500 | 2 379(21) | 342(15) |
| O(11) | 9 139(14) | 1 977(11) | −985(11) |
| O(12) | 9 181(13) | 424(11) | −383(10) |
| O(13) | 9 190(13) | 623(12) | −1 893(10) |
| O(14) | 10 839(12) | 1 063(14) | −1 081(10) |
| O(1) | 3 872(19) | 241(17) | 7 046(16) |
| O(2) | 5 301(39) | 70(34) | 3 924(30) |
| O(21) | 4 026(24) | 1 808(22) | 4 226(20) |
| O(22) | 5 834(35) | 887(30) | 4 201(26) |
| O(23) | 4 000(29) | 245(27) | 3 867(25) |
| O(24) | 4 244(30) | 622(25) | 5 261(23) |

## Results and Discussion

*Discussion of the Structures.*—Bond lengths and angles for the two structures are given in Tables 2 and 3.

The structure of the bromide is analogous to those of most compounds of this type studied previously.[6,11] The $\cdots Br-Pt^{IV}-Br\cdots Pt^{II}\cdots$ chain is completely disordered so that all Pt sites are crystallographically equivalent, and the bromine atom half-occupies two adjacent sites between neighbouring Pt atoms, see Figure 1. The completeness of the chain averaging is well demonstrated by the fact that we were able to identify experimentally, and to refine successfully, the hydrogen atoms on the ammonia ligands.

The $Pt-NH_3$ distances, which are equal within the limits of experimental error, are *ca.* 0.02 Å shorter than those in the anionic chain complex $Cs_2[Pt^{II}(NO_2)(NH_3)X_2][Pt^{IV}(NO_2)$-

**Table 2.** Bond lengths (Å) and angles (°) for the bromide

| | | | |
|---|---|---|---|
| Br–Pt | 2.467(3) | N(1)–Pt–Br | 86.4(3) |
| N(1)–Pt | 2.047(8) | N(2)–Pt–Br | 89.8(3) |
| N(2)–Pt | 2.052(8) | N(2)–Pt–N(1) | 89.9(4) |
| O(1)–S | 1.562(7) | O(2)–S–O(1) | 105.6(5) |
| O(2)–S | 1.432(6) | O(3)–S–O(1) | 107.0(5) |
| O(3)–S | 1.494(6) | O(3)–S–O(2) | 109.6(5) |
| O(4)–S | 1.439(6) | O(4)–S–O(1) | 108.0(6) |
| | | O(4)–S–O(2) | 114.8(5) |
| | | O(4)–S–O(3) | 111.5(5) |
| | | Pt–Br–Pt | 179.9 |

Possible H-bond contacts (Å) *

| | | | |
|---|---|---|---|
| $N(2^{I}) \cdots O(1)$ | 3.05 | $N(1^{III}) \cdots O(3)$ | 2.98 |
| $O(3^{I}) \cdots O(1)$ | 2.57 | $N(1^{IV}) \cdots O(4)$ | 3.10 |
| $N(1^{II}) \cdots O(2)$ | 3.11 | $N(2^{I}) \cdots O(4)$ | 3.14 |
| $N(2^{III}) \cdots O(2)$ | 2.95 | | |

* Symmetry operations: I $-x, -y, -z$; II $1-x, -y, -z$; III $-1+x, \frac{1}{2}-y, -\frac{1}{2}+z$; IV $x, y, z$.

**Table 3.** Bond lengths (Å) and angles (°) for the iodide

| | | | |
|---|---|---|---|
| I(1)–Pt(1) | 3.148(4) | N(21)–Pt(2)–I(1) | 90.4 |
| I(1)–Pt(2) | 2.686(4) | N(22)–Pt(2)–I(1) | 89.6 |
| | | N(23)–Pt(2)–I(1) | 90.7 |
| N(11)–Pt(1) | 2.008(24) | N(24)–Pt(2)–I(1) | 89.3 |
| N(12)–Pt(1) | 2.017(25) | N(22)–Pt(2)–N(21) | 179.2(8) |
| N(13)–Pt(1) | 2.081(22) | N(23)–Pt(2)–N(21) | 93.5(10) |
| N(14)–Pt(1) | 2.094(21) | N(23)–Pt(2)–N(22) | 87.3(9) |
| | | N(24)–Pt(2)–N(21) | 89.5(10) |
| N(21)–Pt(2) | 2.116(21) | N(24)–Pt(2)–N(22) | 89.7(9) |
| N(22)–Pt(2) | 2.064(21) | N(24)–Pt(2)–N(23) | 177.0(9) |
| N(23)–Pt(2) | 2.052(21) | | |
| N(24)–Pt(2) | 2.108(21) | Pt(2)–I(1)–Pt(1) | 179.3(1) |
| | | | |
| O(11)–S(1) | 1.466(14) | O(12)–S(1)–O(11) | 108.4(8) |
| O(12)–S(1) | 1.504(14) | O(13)–S(1)–O(11) | 111.3(9) |
| O(13)–S(1) | 1.429(13) | O(13)–S(1)–O(12) | 105.8(8) |
| O(14)–S(1) | 1.438(13) | O(14)–S(1)–O(11) | 110.1(10) |
| | | O(14)–S(1)–O(12) | 108.9(9) |
| O(21)–S(2) | 1.548(30) | O(14)–S(1)–O(13) | 112.2(9) |
| O(22)–S(2) | 1.491(35) | | |
| O(23)–S(2) | 1.378(32) | O(22)–S(2)–O(21) | 109.9(21) |
| O(24)–S(2) | 1.410(30) | O(23)–S(2)–O(21) | 103.7(20) |
| | | O(23)–S(2)–O(22) | 112.4(21) |
| N(11)–Pt(1)–I(1) | 90.1 | O(24)–S(2)–O(21) | 104.5(19) |
| N(12)–Pt(1)–I(1) | 89.9 | O(24)–S(2)–O(22) | 118.9(21) |
| N(13)–Pt(1)–I(1) | 89.6 | O(24)–S(2)–O(23) | 106.1(22) |
| N(14)–Pt(1)–I(1) | 90.4 | | |
| | | | |
| N(12)–Pt(1)–N(11) | 177.2(10) | | |
| N(13)–Pt(1)–N(11) | 88.9(10) | | |
| N(13)–Pt(1)–N(12) | 88.2(10) | | |
| N(14)–Pt(1)–N(11) | 89.2(10) | | |
| N(14)–Pt(1)–N(12) | 93.6(11) | | |
| N(14)–Pt(1)–N(13) | 178.1(8) | | |

Possible H-bond contacts (Å) *

| | | | |
|---|---|---|---|
| $N(24^{I}) \cdots O(11)$ | 2.90 | $N(14^{V}) \cdots O(14)$ | 3.10 |
| $O(12^{II}) \cdots O(12)$ | 2.55 | $N(21^{VI}) \cdots O(14)$ | 3.12 |
| $N(14^{III}) \cdots O(12)$ | 3.14 | $N(23^{I}) \cdots O(22)$ | 2.94 |
| $N(12^{III}) \cdots O(13)$ | 3.02 | $N(12^{I}) \cdots O(23)$ | 3.08 |
| $N(22^{IV}) \cdots O(13)$ | 2.95 | $N(11^{VII}) \cdots O(24)$ | 2.79 |

* Symmetry operations: I $x, y, z$; II $2-x, -y, -z$; III $-1-x, -y, -z$; IV $\frac{1}{2}+x, -y, -z$; V $-1+x, y, z$; VI $2-x, y, -z$; VII $\frac{1}{2}+x, -y, 1-z$.

$(NH_3)X_4]$, X = Br or I,[12] as would be expected, since we are now dealing with a cationic chain complex. The positive charge on the chain may also be responsible for another interesting difference. The short $Pt^{IV}$–Br bond length of 2.467 Å is also *ca.* 0.02 Å shorter than in the anionic chain of the complex mentioned above, but the $Pt^{II} \cdots Br$ contact distance, of 3.022 Å, is more than 0.3 Å shorter than therein, indicating stronger association within the chain in the cationic chain complex.

The structure of the iodide (Figure 2) also shows this feature with a $Pt^{IV}$–I distance of 2.686 Å (*ca.* 0.02 less than in the caesium salt)[12] and a $Pt^{II} \cdots I$ contact of 3.148 Å, some 0.2 Å shorter. However, the iodide also represents a significant departure from the usual crystal-structure type, in that the $\cdots I\text{–}Pt^{IV}\text{–}I \cdots Pt^{II}$ chain is now completely ordered, with the bridging iodide occupying only one site. Some disorder in the anionic component of the structure has resulted in a lower precision in all atomic positions, so that apparent differences in the average values of $Pt^{IV}$–$NH_3$ and $Pt^{II}$–$NH_3$ bond lengths (2.05 and 2.09 Å, respectively), although interesting, are not strictly significant. Another key difference between the structures of the bromo- and iodo-chains is that, for the former, the $Pt^{II}N_4$ and $Pt^{IV}N_4$ square planes are eclipsed (as required where the chains are disordered), whereas for the latter they are staggered (by 46°) with respect to each other when viewed down the chain axis.

The anionic component of the bromide structure is well defined, with two $[HSO_4]^-$ ions per metal atom. These anions associate into hydrogen-bonded pairs and, although the hydrogen atom could not be located, the S–OH bond is identified as S–O(1), with a length of 1.562 Å. The H-bond acceptor O(3) also gives a slightly lengthened S–O bond of 1.494, which compares with 1.432, 1.439 Å for the other two bonds. The main contacts between these anions and the cationic chain are $O \cdots NH_3$ contacts with distances of 3.05 Å [$O(1) \cdots N(2)$] and greater.

In the iodide, the anionic component is not completely resolved (see Experimental section). The unit cell contains four $I\text{–}Pt^{IV}\text{–}I \cdots Pt^{II}$ chains, which together require 16 balancing negative charges. Eight $[HSO_4]^-$ ions seem to be ordered in one set of general positions, while another set of eight positions seem to be occupied, in a disordered fashion, by four $[SO_4]^{2-}$ ions and one or two single-atom units. This system could comprise either $4 \times ([HSO_4]^- + OH^- + H_2O)$ or $4 \times ([SO_4]^{2-} + 2H_2O)$, both of which will give the necessary charge balance. Unfortunately the disordering is such that we cannot distinguish between the two possibilities.

*Electronic Spectra.*—Large crystals of the mixed-valence complexes are dichroic and have a metallic sheen. The bromide complexes are all dark blue with the electric vector of the incident beam parallel to the needle axis and colourless when it is perpendicular to this axis. The iodide complex is black and brown in these parallel and perpendicular orientations, respectively (Figures 3—5).

The electronic band maxima, obtained by transmission through Nujol mulls or pressed discs, are listed in Table 4, together with the colours of the complexes as crystals and as powders. The strong bands dominating the visible spectrum in each case are assigned to the intervalence $Pt^{IV} \leftarrow Pt^{II}$ transition, by analogy with results on related complexes.[13-18]

*Infrared Spectra.*—The wavenumbers of bands observed in the i.r. spectra and the assignments[19-21] are listed in Table 5. The spectra of the mixed-valence complexes are superpositions of those of the constituent ions, with little or no perturbations on chain formation. They thus require no special comment.

*Resonance-Raman Spectra.*—The resonance-Raman (r.R.) spectra of the complexes (Figures 6—10) are, in all cases

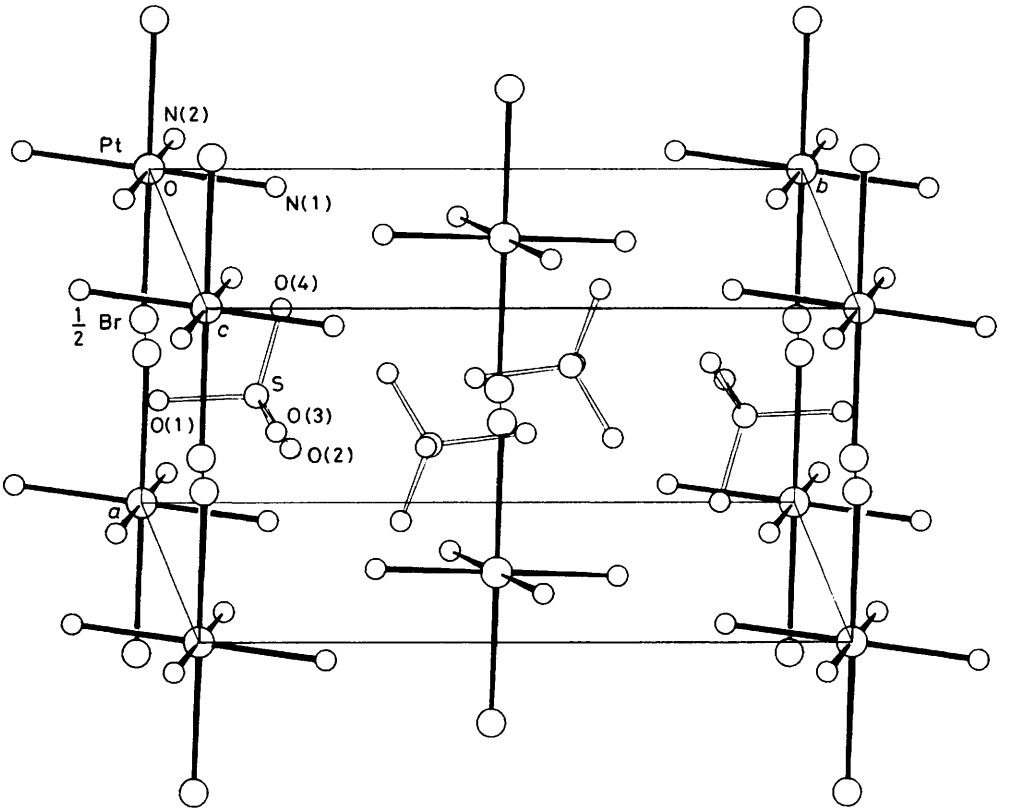


**Figure 1.** Crystal structure of $[Pt(NH_3)_4][Pt(NH_3)_4Br_2][HSO_4]_4$

**Table 4.** Summary of data on complexes studied

| Complex | Crystal [a] | Powder [b] | Mixed-valence max./cm$^{-1}$ | Excitation profile ($\nu_1$) max./cm$^{-1}$ | $\omega_1$/cm$^{-1}$ | $x_{11}$/cm$^{-1}$ | $\frac{I(2\nu_1)}{I(\nu_1)}$ | Progn.[d] |
|---|---|---|---|---|---|---|---|---|
| $[Pt(NH_3)_4][Pt(NH_3)_4Br_2][HSO_4]_4$ | Gold-green | purple | 17 800 [b] | 14 200, 18 300 [c] | 175.6 ±0.3 | −0.42 ±0.03 | 0.58 | $10\nu_1$ |
| $[Pt(NH_3)_4][Pt(NH_3)_4Br_2][ClO_4]_4$ | Gold-green | red | 21 500 [b] | 16 500 | 185.9 ±0.3 | −0.20 ±0.02 | 0.68 | $14\nu_1$ |
| $[Pt(NH_3)_4][Pt(NH_3)_4Br_2][BF_4]_4$ | Gold-green | purple | | 15 000 | 182.6 ±0.3 | −0.22 ±0.03 | 0.44 | $11\nu_1$ |
| $[Pt(NH_3)_4][Pt(NH_3)_4I_2][HSO_4]_3[OH]\cdot H_2O$ | Green-brown | green | 13 600 | < 12 500 | 121.0 ±0.3 | −0.47 ±0.03 | 0.55 | $8\nu_1$ |

[a] By reflection. [b] By transmission. [c] Shoulder. [d] Progn. = progression; at *ca.* 80 K.

studied, dominated by the appearance of a long progression in $\nu_1$, the totally symmetric axial stretching mode, $\nu_{sym}$-(X–$Pt^{IV}$–X), X = Br or I. This progression, as judged from spectra recorded on samples held at *ca.* 80 K, reaches as far as $10\nu_1$, $14\nu_1$, and $11\nu_1$ for the bromo-complexes $[Pt(NH_3)_4][Pt(NH_3)_4Br_2]Y_4$, Y = $HSO_4$, $ClO_4$, or $BF_4$, respectively, and to $8\nu_1$ for the bisulphate salt of the analogous iodo-complex. These results indicate that there is a substantial change (perhaps a few tenths of an Å) in the axial $Pt^{IV}$–X bond length on transition from the ground to the intervalence state. Very much weaker and shorter subsidiary progressions, $v_1\nu_1 + \nu_X$, are also evident in the spectra, *i.e.* progressions in $\nu_1$ built on one quantum of $\nu_X$, where $\nu_X$ is the δ(NPtN) or ν(PtN) mode. The existence of these progressions implies that very slight changes along the $Q_X$ co-ordinates also take place on excitation. The wavenumbers, relative intensities, full widths at half-maxima (f.w.h.m.), and assignments of the bands observed in the various spectra are listed in Tables 6—9.

Figure 9 shows the r.R. spectrum of a single crystal of $[Pt(NH_3)_4][Pt(NH_3)_4Br_2][HSO_4]_4$ in different orientations, when excited with <20 mW of the 568.2 nm line of a $Kr^+$ laser. With the electric vector of the incident beam parallel to the long axis of the crystal (*Z*) and the polariser also parallel to this axis, a resonance spectrum, *Y*(*ZZ*)*X*, is obtained, the characteristic feature of which is the long overtone progression in $\nu_1$. The other three spectra, *Y*(*ZY*)*X*, *Y*(*XY*)*X*, and *Y*(*XZ*)*X*, do not show any strong bands. From this observation it is concluded that the polarisability component $\alpha_{zz}$ is the one which dominates the scattering tensor, and that the intervalence transition is axially (*i.e.* *Z*) polarised. Some Raman studies on this salt have very recently been published [18] but, in particular, the band wavenumbers, polaris-

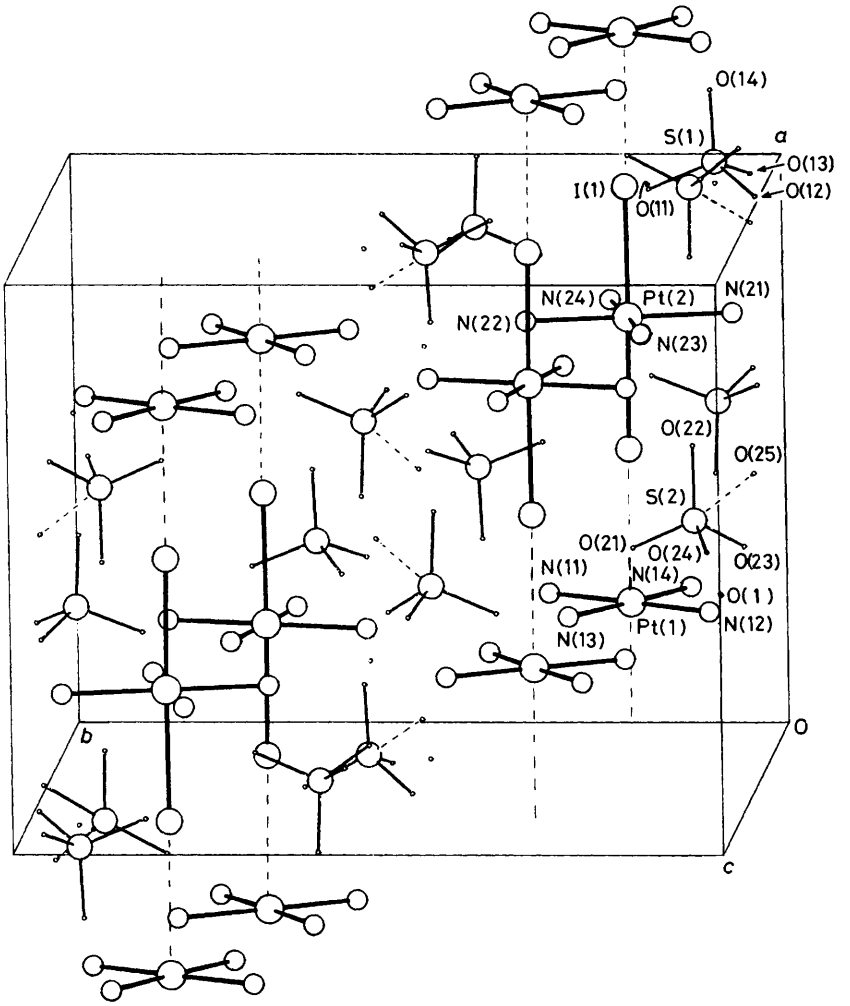


**Figure 2.** Crystal structure of $[Pt(NH_3)_4][Pt(NH_3)_4I_2][HSO_4]_3[OH]\cdot H_2O$

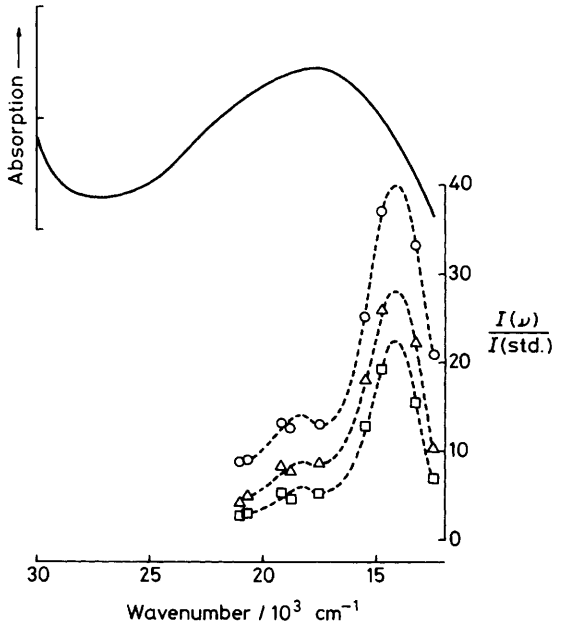


**Figure 3.** Electronic transmission spectrum of $[Pt(NH_3)_4][Pt(NH_3)_4Br_2][HSO_4]_4$ at 295 K together with the excitation profiles of the $\nu_1$ (○), $2\nu_1$ (△), and $3\nu_1$ (□) bands at *ca.* 80 K

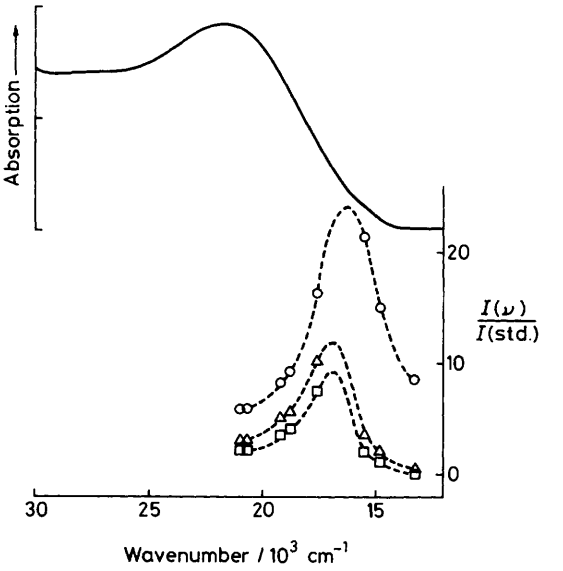


**Figure 4.** Electronic transmission spectrum of $[Pt(NH_3)_4][Pt(NH_3)_4Br_2][ClO_4]_4$ at 295 K and the excitation profiles of the $\nu_1$ (○), $2\nu_1$ (△), and $3\nu_1$ (□) bands at *ca.* 80 K

**Table 5.** Wavenumbers ($cm^{-1}$) of bands observed in the i.r. spectra of the complexes

| | | $[Pt(NH_3)_4][Pt(NH_3)_4Br_2]Y_4$ [c] | | | |
|---|---|---|---|---|---|
| $[Pt(NH_3)_4]Cl_2$ [a] | $[Pt(NH_3)_4Br_2]Br_2$ [b] | Y = $HSO_4$ | Y = $ClO_4$ | Y = $BF_4$ | Assignment [d] |
| 3 250s | | 3 220s,br | 3 310 } s,br | 3 330 } s,br | ν(N–H) |
| 3 140s | 3 150vs | | 3 220 } | 3 230 } | |
| | 3 060vs | | | | |
| 1 560m | 1 558s | 1 570s | 1 600m | 1 600s | $\delta_d(NH_3)$ |
| 1 325s | 1 345vs | 1 335s | 1 335s | 1 330s | $\delta_s(NH_3)$ |
| | | 1 275w | 1 275w | 1 285w | $\omega(NH_2)$ |
| | | 1 220s | | | $\nu_3(HSO_4)$ |
| | | 1 155vs | | | |
| | | | 1 150 (sh) | | $\nu_3(ClO_4)$ |
| | | | 1 075s,br | | |
| | | | | 1 000s,br | $\nu_3(BF_4)$ |
| | | 1 060vs | | | $\nu_1(HSO_4)$ |
| | 935m | | | | |
| 888m | | 854vs | 840m | 846s | $\delta_r(NH_3)$ |
| 842m | | | | | |
| | | 724m | 720m | | |
| | | | | 720s | $\nu_1(BF_4)$ |
| | | | 624s | | $\nu_4(ClO_4)$ |
| | | 609vs | | | $\nu_4(HSO_4)$ |
| | | 583vs | | | |
| | | | | 534s | $\nu_4(BF_4)$ |
| 510w | 516m | 514w | 520w | 521m | ν(Pt–N) |
| | | 470vw | 460m | 480s | |
| | | 430m | | | |
| 236m | 288vs | 278vs | 280s,br | 280s,br | δ(N–Pt–N) |
| | | 258vs,br | | | ν(Pt–Br) |
| | 237s | 242s,br | 242s,br | | $\pi(Pt–N_4)$ |
| 150w | | | | | |
| 118w | 116m | 139m | 100m | | } lattice |
| | 90m | 90m,br | | | |
| | 70w—m | | | | |

[a] Ref. 19. [b] Ref. 20. [c] This work. [d] $\delta_d$ = Degenerate deformation, $\delta_s$ = symmetric deformation.

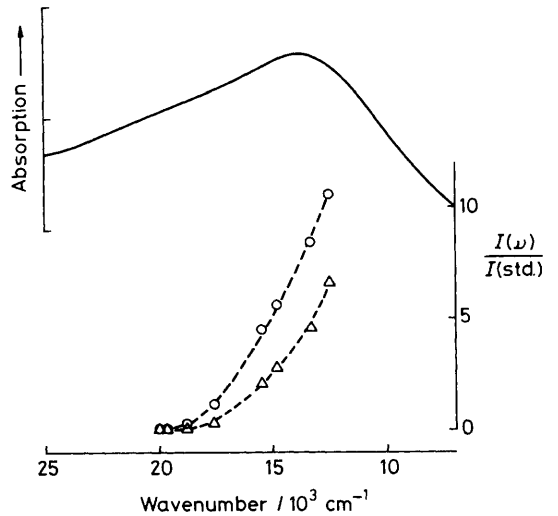


**Figure 5.** Electronic transmission spectrum of $[Pt(NH_3)_4][Pt(NH_3)_4I_2][HSO_4]_3[OH]\cdot H_2O$ at 295 K and the excitation profiles of the $\nu_1$ (○) and $2\nu_1$ (△) bands at *ca.* 80 K

**Table 6.** Wavenumbers, relative intensities, full widths at half-maxima (f.w.h.m.), and assignments of bands observed in the r.R. spectra of $[Pt(NH_3)_4][Pt(NH_3)_4Br_2][HSO_4]_4$

| $\tilde{\nu}/cm^{-1}$ | $I(\nu_i\nu_1)/I(\nu_1)$ | $\Delta\tilde{\nu}_{\frac{1}{2}}/cm^{-1}$ | Assignment |
|---|---|---|---|
| 174.6 | 1.00 | 10.6 | $\nu_1(Br–Pt^{IV}–Br)_{sym}$ |
| 213.9 | | | δ(N–Pt–N) |
| 348.4 | 0.58 | 19.7 | $2\nu_1$ |
| 388.3 | | | $\nu_1$ + δ(N–Pt–N) |
| 521.0 | 0.42 | 32 | $3\nu_1$ |
| 556 | | | ν(Pt–N) |
| 694.4 | 0.28 | 39 | $4\nu_1$ |
| 730 | | | $\nu_1$ + ν(Pt–N) |
| 865.1 | 0.22 | 52 | $5\nu_1$ |
| 1 037.7 | 0.15 | 60 | $6\nu_1$ |
| 1 206 | 0.10 | 71 | $7\nu_1$ |
| 1 369 | 0.07 | 87 | $8\nu_1$ |
| 1 542 | 0.05 | 105 | $9\nu_1$ |
| 1 710 | *ca.* 0.03 | *ca.* 120 | $10\nu_1$ |

Obtained with 647.1-nm excitation at *ca.* 80 K, as a $K_2SO_4$ disc.

ations, and assignments differ in many respects from those found here. The present spectra, taken at all four polarisations (rather than just two), are clear-cut and well defined.

The observation of long overtone progressions in a r.R. spectrum permits [12] the calculation of the anharmonicity constant $x_{11}$ and of an approximate value for the harmonic wavenumber, $\omega_1$. The results of these analyses of the spectral data are included in Table 4. It is clear that in all cases, $\nu_1$, the progression-forming mode, behaves almost exactly as a simple harmonic oscillator, even out as far as $14\nu_1$, and thus that the appropriate potential well is almost exactly parabolic near its minimum.

The excitation profiles (plots of Raman band intensities *versus* excitation wavenumber) of the $\nu_1$ band and its first two

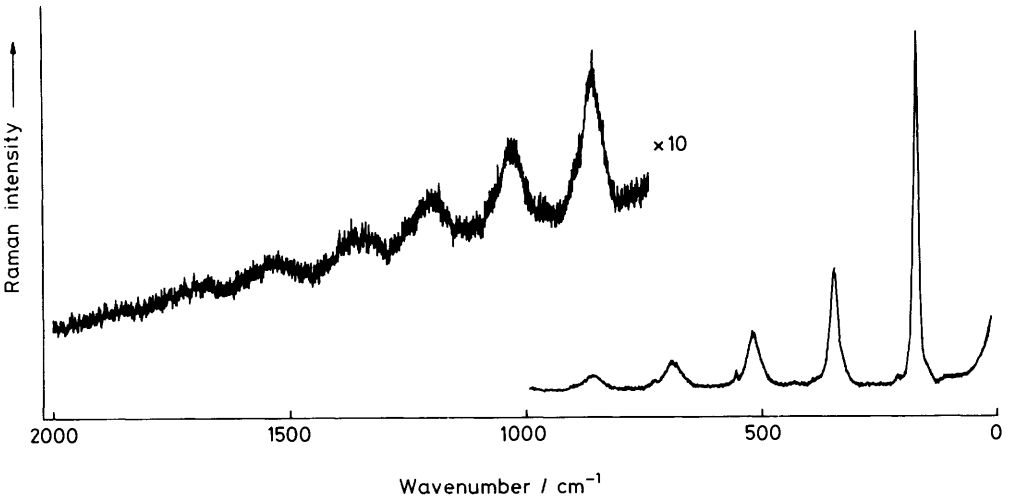


**Figure 6.** Resonance-Raman spectum of $[Pt(NH_3)_4][Pt(NH_3)_4Br_2][HSO_4]_4$ as a $K_2SO_4$ disc at *ca.* 80 K ($\lambda_0$ = 647.1 nm, slit width *ca.* 2 $cm^{-1}$)

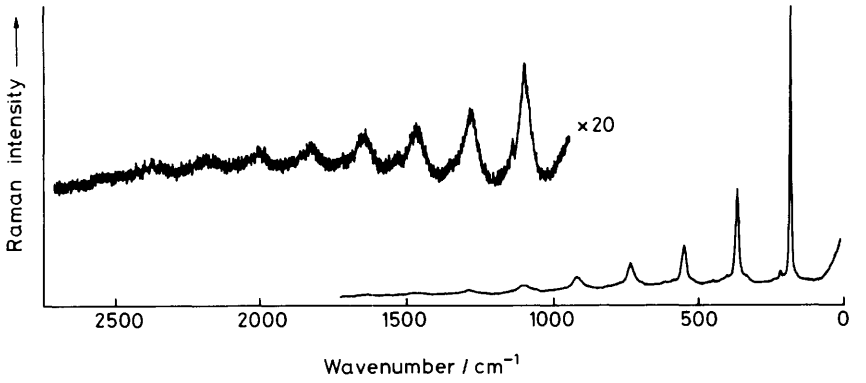


**Figure 7.** Resonance-Raman spectrum of $[Pt(NH_3)_4][Pt(NH_3)_4Br_2][ClO_4]_4$ as a $K_2SO_4$ disc at *ca.* 80 K ($\lambda_0$ = 530.9 nm, slit width *ca.* 2 $cm^{-1}$)

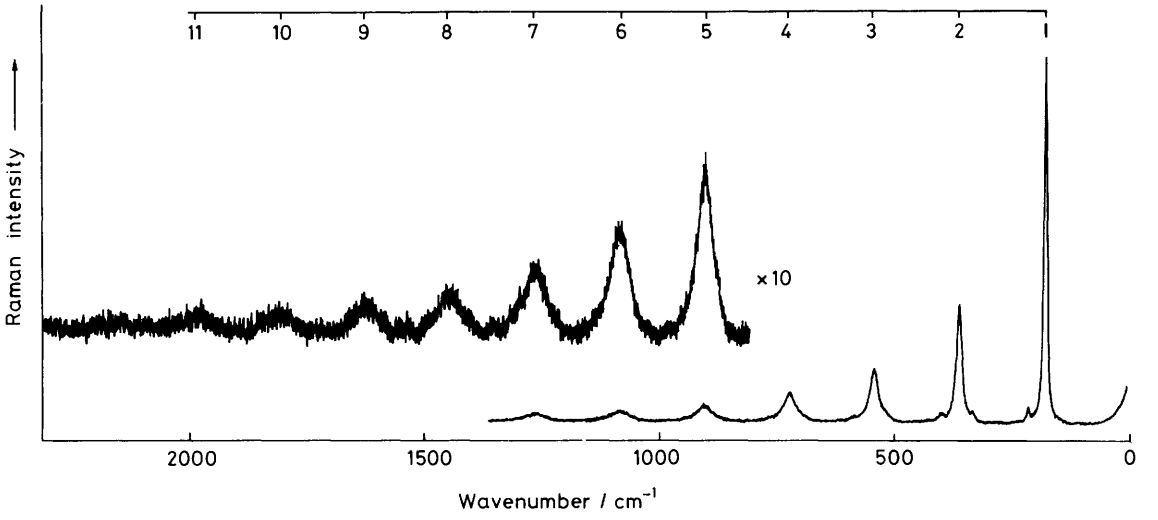


**Figure 8.** Resonance-Raman spectrum of $[Pt(NH_3)_4][Pt(NH_3)_4Br_2][BF_4]_4$ as a $K_2SO_4$ disc at *ca.* 80 K ($\lambda_0$ = 568.2 nm, slit width *ca.* 1.5 $cm^{-1}$). The upper scale indicates the vibrational quantum numbers for the $\nu_1$ mode

**Table 7.** Wavenumbers, relative intensities, f.w.h.m., and assignments of bands observed in the r.R. spectrum of $[Pt(NH_3)_4][Pt(NH_3)_4Br_2][ClO_4]_4$

| $\tilde{\nu}$/cm$^{-1}$ | $I(\nu_1\nu_1)/I(\nu_1)$ | $\Delta\tilde{\nu}_{\frac{1}{2}}$/cm$^{-1}$ | Assignment |
|---|---|---|---|
| 184.7 | 1.00 | 6.3 | $\nu_1(Br-Pt^{IV}-Br)_{sym}$ |
| 219.5 | | | $\delta(N-Pt-N)$ |
| 370.6 | 0.68 | 12.6 | $2\nu_1$ |
| 405.9 | | | $\nu_1 + \delta(N-Pt-N)$ |
| 555.2 | 0.51 | 19.7 | $3\nu_1$ |
| 740.0 | 0.40 | 26 | $4\nu_1$ |
| 924.4 | 0.30 | 33 | $5\nu_1$ |
| 1 106.1 | 0.25 | 39 | $6\nu_1$ |
| 1 289.6 | 0.20 | 50 | $7\nu_1$ |
| 1 472.4 | 0.15 | 63 | $8\nu_1$ |
| 1 658 | 0.10 | 72 | $9\nu_1$ |
| 1 837 | 0.07 | 85 | $10\nu_1$ |
| 2 015 | 0.05 | 100 | $11\nu_1$ |
| 2 200 | *ca.* 0.03 | >100 | $12\nu_1$ |
| 2 380 | <0.03 | >100 | $13\nu_1$ |
| 2 555 | <0.03 | >100 | $14\nu_1$ |

Obtained with 530.9-nm excitation at *ca.* 80 K, as $K_2SO_4$ disc.

**Table 8.** Wavenumbers, relative intensities, f.w.h.m., and assignments of bands observed in the r.R. spectrum of $[Pt(NH_3)_4][Pt(NH_3)_4Br_2][BF_4]_4$

| $\tilde{\nu}$/cm$^{-1}$ | $I(\nu_1\nu_1)/I(\nu_1)$ | $\Delta\tilde{\nu}_{\frac{1}{2}}$/cm$^{-1}$ | Assignment |
|---|---|---|---|
| 181.7 | 1.00 | 6.7 | $\nu_1(Br-Pt^{IV}-Br)_{sym}$ |
| 218.7 | | | $\delta(N-Pt-N)$ |
| 336.4 | | | |
| 364.3 | 0.44 | 9.5 | $2\nu_1$ |
| 403.1 | | | $\nu_1 + \delta(N-Pt-N)$ |
| 519 | | | $\nu_1 + 336.4$ |
| 545.7 | 0.35 | 16.5 | $3\nu_1$ |
| 587 | | | $2\nu_1 + \delta(N-Pt-N)$ |
| 726.7 | 0.34 | 30.7 | $4\nu_1$ |
| 908.1 | 0.27 | 39 | $5\nu_1$ |
| 1 088.4 | 0.19 | 45 | $6\nu_1$ |
| 1 267 | 0.14 | 55 | $7\nu_1$ |
| 1 447 | 0.12 | 60 | $8\nu_1$ |
| 1 626 | 0.09 | 70 | $9\nu_1$ |
| 1 800 | 0.06 | 80 | $10\nu_1$ |
| 1 980 | *ca.* 0.03 | >80 | $11\nu_1$ |

Obtained with 568.2-nm excitation at *ca.* 80 K, as a $K_2SO_4$ disc.

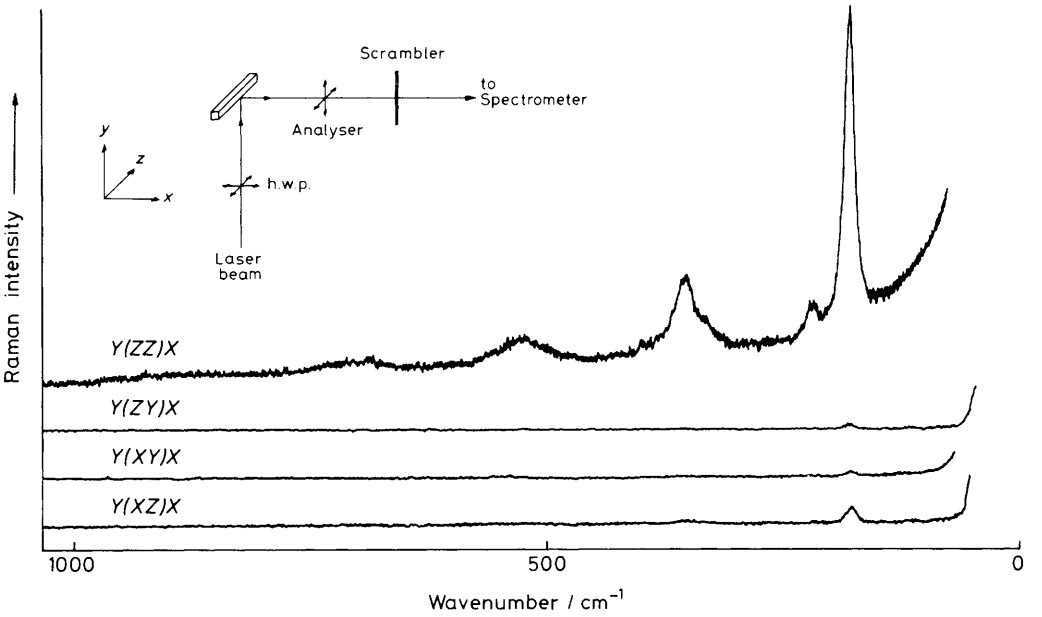


**Figure 9.** Resonance-Raman spectrum of an oriented single crystal of $[Pt(NH_3)_4][Pt(NH_3)_4Br_2][HSO_4]_4$ at 293 K ($\lambda_0$ = 568.2 nm, slit width *ca.* 2 cm$^{-1}$). A half-wave plate (h.w.p.) is used to rotate the direction of polarisation of the incident beam by 90°

overtones for two of the bromo-complexes and for the iodo-complex are included in Figures 3—5. All the excitation profiles maximise 3 000—4 000 cm$^{-1}$ to the low-wavenumber side of the maximum of the resonant intervalence band (although still within its contour) in each case, a feature which has proved to be typical of linear-chain mixed-valence complexes,[11-17] and especially of those possessing semiconductor properties.

## Conclusion

Amongst the products of the oxidation of Magnus green, in the presence of KBr or KI, it is now certain that linear-chain halogen-bridged species of the sort $[Pt(NH_3)_4][Pt(NH_3)_4X_2]Y_4$, where X = Br or I and Y may be $HSO_4$, $ClO_4$, or $BF_4$, occur. These complexes are directly analogous to the many other linear-chain complexes of platinum now reported upon and studied. Other products of the reactions are also evident, and further work in this area is necessary in order better to define the intermediates between Magnus-green-type structures and those reported in this paper.

## Acknowledgements

The authors thank the Science Research Council and the University of London for financial support, and Johnson

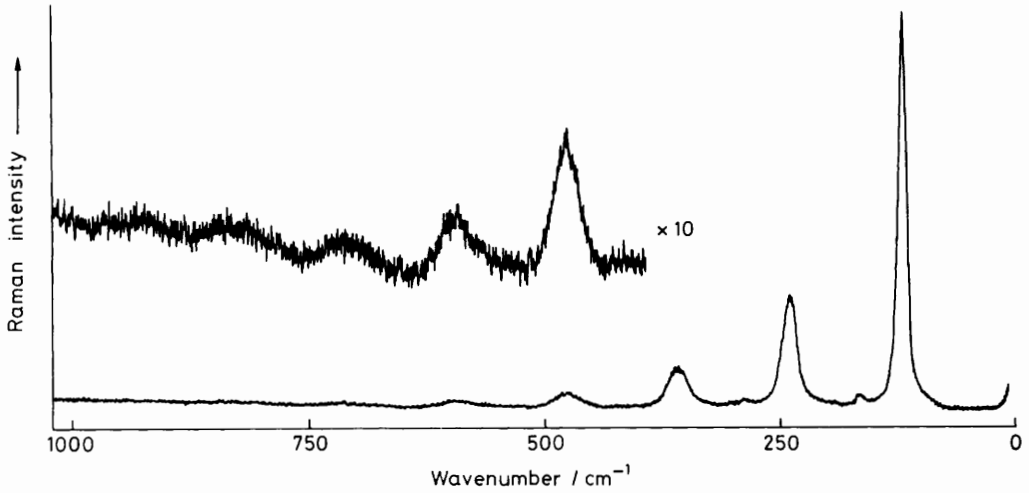


**Figure 10.** Resonance-Raman spectrum of $[Pt(NH_3)_4][Pt(NH_3)_4I_2][HSO_4]_3[OH]\cdot H_2O$ as a $K_2SO_4$ disc at *ca.* 80 K ($\lambda_0$ = 676.4 nm, slit width 1 $cm^{-1}$)

**Table 9.** Wavenumbers, relative intensities, and f.w.h.m. of bands observed in the r.R. spectrum of $[Pt(NH_3)_4][Pt(NH_3)_4I_2][HSO_4]_3\cdot[OH]\cdot H_2O$

| $\tilde{\nu}/cm^{-1}$ | $I(\nu_1\nu_1)/I(\nu_1)$ | $\Delta\tilde{\nu}_{\frac{1}{2}}/cm^{-1}$ | Assignment |
|---|---|---|---|
| 119.4 | 1.00 | 9.8 | $\nu_1$ |
| 164.1 | | | |
| 238.9 | 0.55 | 18.5 | $2\nu_1$ |
| 286 | | | $\nu_1 + 164.1$ |
| 357.4 | 0.26 | 24 | $3\nu_1$ |
| 475.2 | 0.15 | 33 | $4\nu_1$ |
| 589.6 | 0.10 | 43 | $5\nu_1$ |
| 705 | 0.04 | 55 | $6\nu_1$ |
| 820 | *ca.* 0.02 | *ca.* 70 | $7\nu_1$ |
| 925 | <0.02 | >70 | $8\nu_1$ |

Obtained as a $K_2SO_4$ disc at *ca.* 80 K with 676.4-nm excitation.

Matthey Ltd. for a loan of chemicals. M. K. thanks the Department of Chemistry, University College London, for a studentship.

## References

1 J. S. Miller and A. J. Epstein (eds.), *Ann. N.Y. Acad. Sci.*, 1978, 313, 481—701.
2 ' Low Dimensional Cooperative Phenomena,' ed. H. J. Keller, Plenum, New York, 1974.
3 ' Chemistry and Physics of One Dimensional Metals,' ed. H. J. Keller, Plenum, New York, 1977.
4 ' Molecular Metals,' ed. W. E. Hatfield, NATO Conference Series, Plenum, New York, 1978.
5 ' Mixed-Valence Compounds,' ed. D. B. Brown, D. Reidel, Dordrecht, 1980.
6 R. J. H. Clark, in ref. 5, p. 271.
7 G. C. Papavassiliou and T. Theophanides, *Z. Naturforsch., Teil B*, 1979, **34**, 986.
8 W. Kiefer, in 'Advances in Infrared and Raman Spectroscopy,' eds. R. J. H. Clark and R. E. Hester, Heyden, London, 1977, vol. 3, p. 1.
9 R. J. H. Clark, in 'Advances in Infrared and Raman Spectroscopy,' eds. R. J. H. Clark and R. E. Hester, Heyden, London, 1975, vol. 1, p. 143.
10 M. B. Hursthouse, R. A. Jones, K. M. A. Malik, and G. Wilkinson, *J. Am. Chem. Soc.*, 1979, **101**, 4128.
11 R. J. H. Clark, *Ann. N.Y. Acad. Sci.*, 1978, **313**, 672.
12 R. J. H. Clark, M. Kurmoo, A. M. R. Galas, and M. B. Hursthouse, *Inorg. Chem.*, 1981, **20**, 4206.
13 R. J. H. Clark and P. C. Turtle, *Inorg. Chem.*, 1978, **17**, 2526.
14 R. J. H. Clark and M. Kurmoo, *Inorg. Chem.*, 1980, **19**, 3522.
15 R. J. H. Clark, M. Kurmoo, H. J. Keller, B. Keppler, and U. Traeger, *J. Chem. Soc., Dalton Trans.*, 1980, 2498.
16 R. J. H. Clark and M. Kurmoo, *J. Chem. Soc., Dalton Trans.*, 1981, 524.
17 J. R. Campbell, R. J. H. Clark, and P. C. Turtle, *Inorg. Chem.*, 1978, **17**, 3622.
18 D. Layek and G. C. Papavassiliou, *Z. Naturforsch., Teil B*, 1981, **36**, 83.
19 H. Poulet, P. Delorme, and J. P. Mathieu, *Spectrochim. Acta*, 1964, **20**, 1855.
20 D. W. James and M. J. Nolan, *J. Raman Spectrosc.*, 1973, **1**, 271.
21 J. Hiraishi, I. Nakagawa, and T. Shimanouchi, *Spectrochim. Acta, Part A*, 1968, **24**, 819.

*Received* 26*th April* 1982; *Paper* 2/681